Electrostatic Precipitators - Modelling and Analytical Verification Concept

Donato Rubinetti[1], Daniel A. Weiss[1] and Walter Egli[2]

***Abstract*—The numerical model in this work for a simple wire-tube configuration electrostatic precipitator (ESP) is based on Navier-Stokes and Maxwell's equations. The connection between Fluid Dynamics and Electrostatics is established through the forces exerted on charged particles, namely Drag- and Coulomb-forces. The simulations are carried out using the commercial code COMSOL Multiphysics. The air ionization by corona discharge is described by coupling Poisson's equation with the continuity equation for space charge density. The corresponding boundary condition for the emitting electrode relates the electric field to the space charge density. This analysis provides a robust and computational time efficient approach for calculating the initial space charge density on the electrode using the current density as fitting parameter.**
Results for the electric field and the space charge density have been analytically verified.

***Keywords*—Corona Discharge, Electrostatic Precipitation, Charge Density, Charge Conservation.**

I. Introduction

Electrostatic precipitation is a reliable technology to control emissions of airborne particles in series of applications such as coal-fired power plants, cement plants or even for domestic fireplaces. Particle removal is of international interest, e.g. a key point of the European Union's energy politics is the generation of power from renewable resources such as wood-burning [1]. Thus, an efficient particle removing device for exhaust gases treatment is needed. Numerical calculations allowed for further developments of ESP's avoiding test stands and field tests.

II. Physical Model

The physical model for the fluid dynamics part is based on incompressible Navier-Stokes equations in steady-state conditions. The resulting velocity field is used into Schiller-Naumann's Drag model for particle motion. For submicron-diameter particles the drag force is corrected by the Cunningham factor, which bridges the gap between molecular and continuum limit [2].
The second major force acting on particles is the Coulomb force which is the product of particle charge and the surrounding electric field. Whereas the time- respectively location-dependent particle charge processes can be described by diffusion- and field-charging effects, the electrostatic part needs careful consideration. Derived from Maxwell's equations, assuming stationary conditions and neglecting magnetic influence the following equations need to be fulfilled at every point of the computational domain for the electrostatic part:

$$\nabla \cdot \vec{E} = \frac{\rho_{el}}{\varepsilon_0} \tag{1}$$

$$\vec{E} = -\nabla\phi \tag{2}$$

with charge conservation

$$\nabla \cdot \vec{j} = 0 \tag{3}$$

and

$$\vec{j} = \rho_{el}(\vec{w} + b\vec{E}) - D_c \nabla \rho_{el}. \tag{4}$$

With electric field $\vec{E}$, space charge density ρ_{el}, vacuum permittivity ε_0, electric potential ϕ, current density $\vec{j}$, velocity field $\vec{w}$, ion mobility b and diffusion constant D_c. Equation (1) combines with equation (2) to Poisson's equation

$$\nabla^2\phi = -\frac{\rho_{el}}{\varepsilon_0}. \tag{5}$$

Neglecting diffusive and convective effects in equation (3) and (4) yields the second partial differential equation (PDE)

$$\vec{E}\nabla\rho_{el} = -\frac{{\rho_{el}}^2}{\varepsilon_0}. \tag{6}$$

These PDEs are suited to describe the Corona discharge problem. The air ionization process is taken into consideration rather on a macroscopic scale than on molecular level by setting a boundary condition on the emitting electrode for $\vec{E}$ and ρ_{el}.

III. Simulations

Corona discharge problems have been numerically investigated by various industry researchers with specific codes such as ABB [4]. However, for time- and cost-efficient purposes a stable approach with the commercial tool COMSOL Multiphysics is proposed, which conveniently offers an interface for defining customized PDEs.

A. General Setup

The simulation is structured within three studies as follows:

1) Stationary fluid flow simulation using CFD module - Turbulent Flow SST
2) Stationary electrostatics simulation using Electrostatics and PDE interface
3) Time-dependent particle motion using Particle Tracing for Fluid Flow Module

[1]Institute of Thermal- and Fluid-Engineering of the University of Applied Sciences Northwestern Switzerland, Klosterzelgstrasse 2, 5210 Windisch (CH) e-mail: donato.rubinetti@fhnw.ch, daniel.weiss@fhnw.ch
[2]EGW Software Engineering, http://egw.egli1.ch/

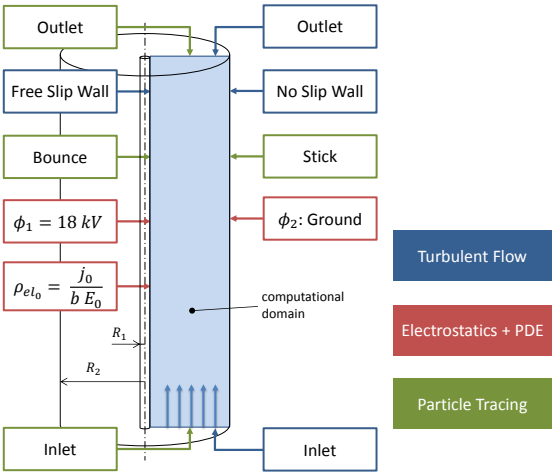

Fig. 1: Boundary Conditions of the 2D-Axissymmetric case for all studies.

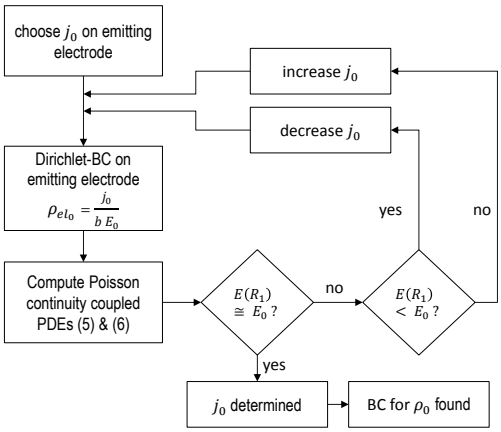

Fig. 2: User-operated iteration scheme for obtaining the space charge density on the electrode ρ_0 with the current density j_0 as fitting parameter.

B. Computation Domain

The boundary conditions for the complete setup are illustrated by figure 1. The geometry is a 2D-axisymmetric wire-tube configuration. Particular attention is given to the space charge density on the electrode, which is determined by the user-operated iteration scheme as shown in figure 2. A fully coupled solution has been proposed by Favre [3] by splitting the space charge density in a constant and space-dependent component. However, this concept has proven to be too delicate for submicrometer emitting electrodes. Instead in this work the current density j_0 is used as fitting parameter, with a very simple relation:

$$\rho_{el_0} = \frac{j_0}{bE_0}. \tag{7}$$

Where E_0 is the Corona onset field strength known as Peek-Kaptzov condition, which assumes that the electric field strength on the electrode remains constant after reaching the critical value. The required field strength E_0 in $[V/m]$ for a wire-tube ESP configuration is calculated as follows [5]

$$E_0 = 3 \times 10^6 f_r \left(m_s + 0.03\sqrt{\frac{m_s}{R_1}} \right). \tag{8}$$

Where f_r is a dimensionless fatigue estimation ($f_r = 0.6$ for practical use), m_s denotes the relative gas density and d_e the emitting electrode diameter.

C. Mesh

The computational mesh consists of mapped elements with refinements to the inner and outer electrode. As shown in figure 3, the ratio from first cell thickness and inner electrode δ/R_1 equals 0.4 which ensures a reliable representation of the high gradients of the electric field in this area.

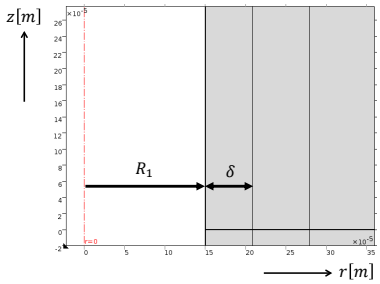

Fig. 3: Cutout of the 2D-Axissymmetric geometry and the corresponding computational mesh.

D. Results

1) Study 1 - fluid flow: The computed fluid flow is illustrated by figure 4 which shows the characteristic velocity profile of a fully developed turbulent profile. As the emitting electrode is assumed to be unaffected by the flow, the velocity reaches its peak value in the emitting electrode region. Thus, no further validation for the fluid flow part is needed as the results match literature findings.

2) Study 2 - electrostatics: The results for the electrostatic part are represented by figure 6 and 7, respectively. The numerical and analytical solutions for the electric field and space charge density along the radial coordinate coincide.

3) Study 3 - particle motion: The results for particle motion are represented in figure 5 for a range of particle diameters between $0.001 - 10\mu m$. As expected, the smallest particles are deposited firstly as they barely experience any drag force. Secondly, the biggest particles are deposited due to their capability of holding higher charge which leads to a greater Coulomb force. Particles of intermediate size are the most difficult to deposit.

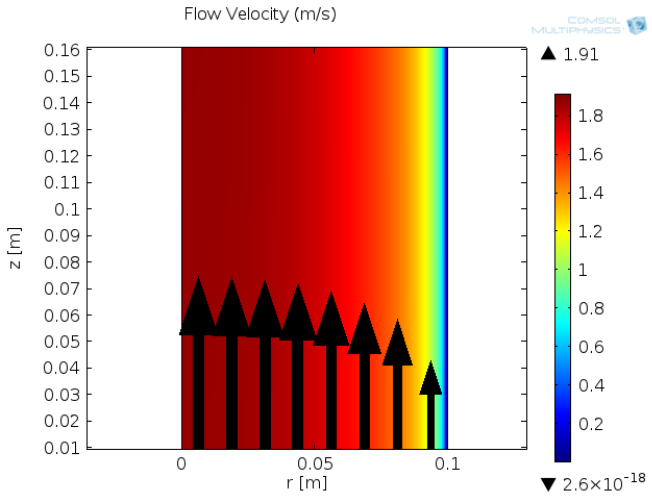

Fig. 4: Study 1 solution for the fluid flow - the fully developed velocity profile.

IV. Analytical Verification

For analytical verification of the wire-tube ESP test case the following dimensionless distributions of the electric field and space charge density along the radial component of the innerspace between the two electrodes have been derived [6]:

$$\frac{E(r)}{E_0} = \hat{E} = \frac{1}{\hat{r}}\sqrt{1 + \hat{A}(\hat{r}^2 - 1)} \tag{9}$$

$$\frac{\rho_{el}(r)}{\frac{\varepsilon_0 E_0}{R_1}} = \hat{\rho}_{el} = \frac{\hat{A}}{\sqrt{1 + \hat{A}(\hat{r}^2 - 1)}} \tag{10}$$

with the dimensionless radius $\hat{r} = r/R_1$ and the dimensionless current $\hat{A}$

$$\hat{A} = \frac{j_0 R_1}{\varepsilon_0 b E_0^2}. \tag{11}$$

As shown by the plots in figures 6 and 7 the numerical and analytical solutions are identical.

V. Conclusion

The approach presented in this paper features a complete setup of an ESP including a robust semi-coupled iteration scheme for calculating the space charge density on the emitting electrode. As the results for the electrostatic study have been analytically verified, the modelling concept can be extended to other cases.

Additionally, the present modelling concept was used for a reconstruction of the calculations and measurements conducted by Meyer *et al.* [7, 8]. Whereas numerical results are obtained easily, the comparison with experimental data diverges due to the lack of accuracy of measurement devices - since the electric field close to the emitting electrode experiences high gradients within sub-millimeter scales, experimental data is too delicate to obtain.

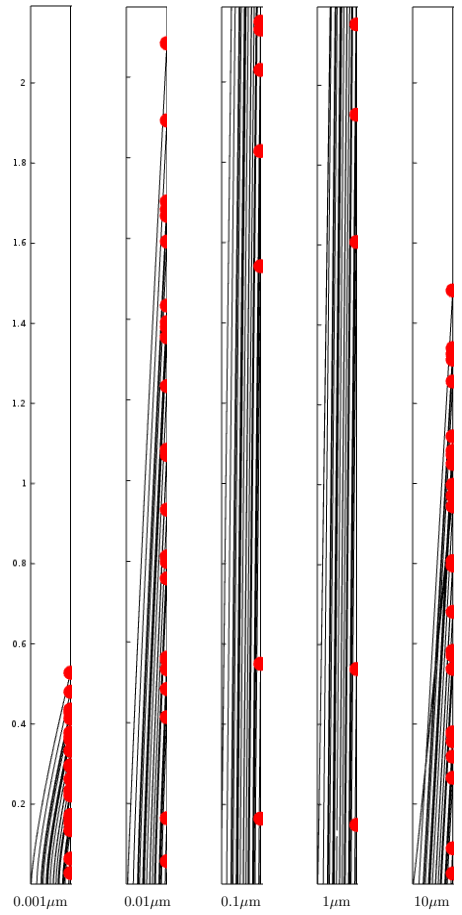

Fig. 5: Study 3 solution for the particle motion - this section of the ESP shows the particle trajectories for five different particle sizes.

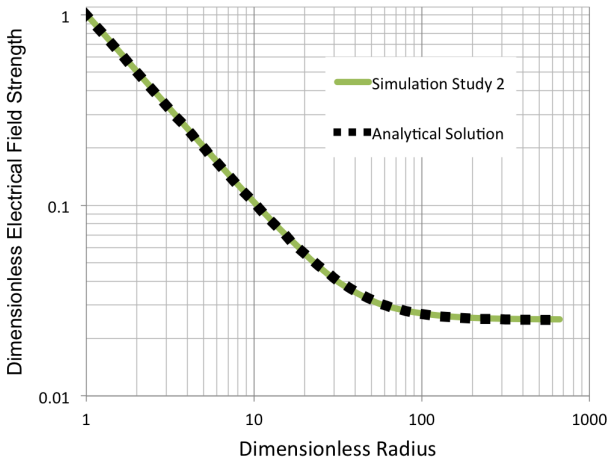

Fig. 6: Analytical verification of the electric field strength.

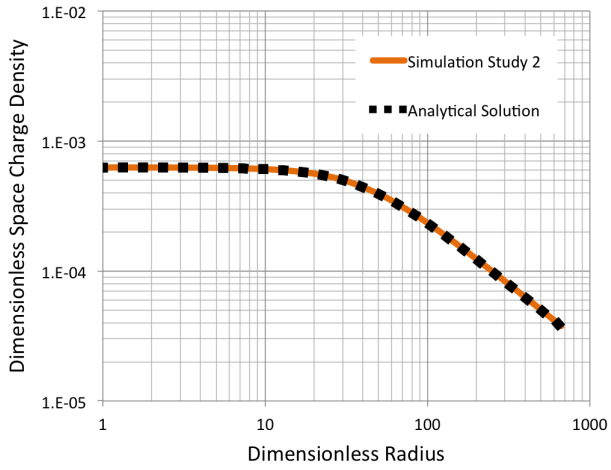

Fig. 7: Analytical verification of the space charge density.

Further investigation on cone-shaped electrode needles, where the tip of the needle is emitting has been successfully conducted. The robust, user-operated iteration algorithm has proven to be suitable also for convection- and diffusion-affected cases. For this project COMSOL Multiphysics has been chosen due to its capability of including user-defined custom PDEs in a coupled manner.

REFERENCES

[1] European Commission, Directorate-General for Climate Action (2014): *The 2020 climate and energy package*. https://ec.europa.eu/energy/en/topics/energy-strategy/2020-energy-strategy , Accessed on 2015-08-20

[2] Hinds, William C. (1999): *Aerosol technology - properties, behavior, and measurements of airborne particles.* 2nd edition. New York: John Wiley & Sons

[3] Favre, Eric (2013): *Corona with details*. http://www.comsol.com/community/forums/general/thread/14399, Accessed on 2015-08-24

[4] Kogelschatz, U.; Egli, W.; Gerteisen, Edgar A. (1999): *Advanced computational tools for electrostatic precipitators*. ABB Review, Volume 4/1999, p.33-42.

[5] White, Harry J. (1963): *Industrial electrostatic precipitation*. Oxford: Pergamon

[6] Weiss, D. A. (2014): *Notes on Electrostatics and Fluidmechanics*. Windisch: University of Applied Sciences Northwestern Switzerland

[7] Meyer, J.; Marquard, A.; Poppner, M.; Sonnenschein, R. (2005): *Electric Fields coupled with ion space charge. Part 1: measurements*, Journal of Electrostatics, Volume 63, p. 775-780.

[8] Meyer, J.; Poppner, M.; Sonnenschein, R. (2005): *Electric Fields coupled with ion space charge. Part 2: computation*, Journal of Electrostatics, Volume 63, p. 781-787.